

Research Paper

Examining the Impacts of Urban Expansion on Spatial Patterns of Rurban Space Case Study: Urmia City

Abolfazl Ghanbari ^{1*}, Amin Khalili ², Bakhtiar Feizizadeh ³

Department of GIS, Faculty of Geography and Planning, University of Tabriz, Tabriz, Iran

Received: October 2024, Revised: September 2025, Accepted: October 2025, Publish Online: October 2025

Abstract

Urban expansion in medium-sized cities of the Global South, though often overlooked, has significant ecological and social implications. This study examines Urmia (a city in Iran) over three decades (1990–2020) using Landsat imagery to quantify urban growth through spatial metrics (UEII, UEDI) and Geographically Weighted Regression (GWR) to explore the spatiotemporal patterns of expansion. The analysis reveals that built-up areas increased from 2.7% to 8.7%, with a marked concentration at the urban periphery. Fragmentation of land, agricultural conversion, and shrinking water bodies highlight the emergence of a "Rurban" landscape. Spatially varying relationships identified through GWR suggest that expansion intensity is closely linked to landscape configuration. The findings emphasize the urgent need for infill development and sustainable land management to curb peripheral sprawl and promote more balanced urban growth. Urban expansion in medium-sized cities of the Global South remains an underexplored topic despite its growing ecological, social, and economic impacts. This study investigates the spatiotemporal dynamics of urban growth in Urmia (Iran) from 1990 to 2020 using Landsat imagery and a combination of spatial metrics, including the Urban Expansion Intensity Index (UEII) and Urban Expansion Density Index (UEDI). Additionally, Geographically Weighted Regression (GWR) is applied to identify spatially varying relationships between expansion intensity and landscape features. The findings reveal a substantial increase in built-up areas, from 2.7% in 1990 to 8.7% in 2020, with growth primarily concentrated at the urban periphery. This expansion led to the fragmentation of land, conversion of agricultural areas, and significant environmental changes, including a reduction in water bodies. The results show that the intensity of urban expansion is strongly linked to fragmentation and spatial isolation, highlighting the emergence of a "Rurban" landscape—where urban and rural patterns increasingly blend. GWR analysis reveals that spatial relationships between growth and landscape configuration vary significantly across the study area, indicating the complex nature of urban dynamics. These findings emphasize the need for strategic urban planning that prioritizes infill development and sustainable land management to prevent further urban sprawl and promote more balanced growth. The study contributes new insights into the understanding of urban expansion in regions with limited data and offers valuable implications for future urbanization policies in similar settings.

Keywords: Urban expansion, Landscape patterns, Geographic spatial regression, Geographic information system, Urmia.

* Corresponding author: a_ghanbari@tabrizu.ac.ir
© 2025 Iran University of Science & Technology.

INTRODUCTION

Urbanization has emerged as one of the defining processes of the 21st century, profoundly reshaping ecological systems, social structures, and economic trajectories worldwide (Wu et al., 2016; Rimal et al., 2017). Over the last seven decades, the proportion of the global population residing in urban areas has grown from less than one-third in 1950 to more than half today, and it is projected to reach 66% by 2050 (Huang et al., 2019). Beyond its demographic magnitude, the nature of urban expansion, whether compact, polycentric, fragmented, or sprawling, has become a central concern for urban geography and sustainability debates. While urban growth is often linked with economic opportunity and improved access to infrastructure, the form and spatial configuration of expansion determine whether its consequences are beneficial or detrimental to ecological resilience and social equity. Thus, the question is not only how much cities grow, but *how* they grow.

Most empirical and theoretical studies of urban expansion have focused on metropolitan regions in North America, Europe, and East Asia. These contexts have provided a wealth of insights into concepts such as suburbanization, peri-urbanization, compact city strategies, and landscape urbanism (Zhao et al., 2019; You & Yang, 2017). However, the trajectories of urbanization in the Global South differ substantially, shaped by weaker institutional capacity, rapid demographic pressures, environmental vulnerabilities, and limited planning frameworks. Within this vast literature, secondary or medium-sized cities remain significantly underexplored, despite their pivotal role in absorbing a growing share of the urban population (Terfa et al., 2020; Al Rifat & Liu, 2019). Scholars increasingly emphasize that overlooking medium-sized cities risks ignoring some of the most pressing sustainability challenges, as these cities often experience faster

and less regulated growth than megacities (Seto et al., 2022; Jones & Kuffer, 2023).

In Iran, research on urban expansion has concentrated predominantly on Tehran and a few other major metropolitan centers (Assari et al., 2016; Madanian et al., 2018). Yet medium-sized cities across the country are undergoing rapid transformation. Their expansion often outpaces planning institutions, leading to fragmented development, ecological degradation, and socio-spatial inequality (Pourafkari et al., 2018; Sidi, 2018). This imbalance underscores a clear research gap: the dynamics of urbanization in medium-sized Iranian cities have not been systematically documented, even though these cities collectively account for a significant portion of national urban growth. Moreover, secondary cities are central to achieving global policy agendas such as Sustainable Development Goal 11 (Sustainable Cities and Communities) and climate change adaptation, but their role remains underacknowledged in both scholarship and planning practice.

The city of Urmia, located in West Azerbaijan Province, provides a compelling case to investigate these dynamics. With a population exceeding 700,000, Urmia has expanded rapidly since the 1990s in parallel with agricultural decline, industrial restructuring, and the ecological crisis of Lake Urmia. The expansion of built-up areas has come at the cost of fertile agricultural land, vegetation cover, and surface water resources. These changes resonate with global concerns about peri-urban sprawl, food security, and ecological vulnerability (Seto et al., 2012; Karimi et al., 2019). The transformation of Urmia illustrates the tension between urban development and environmental resilience in secondary cities, highlighting how weak institutional capacity exacerbates ecological stress.

Conceptually, it is also important to consider how transitional landscapes are framed. Internationally, the terms *peri-urban* or *suburban*

are commonly used to describe areas at the urban fringe where rural and urban activities overlap. In Iranian planning discourse, however, the notion of *rurban space* has gained prominence. Unlike peri-urban, which emphasizes transitional dynamics, *rurban* highlights hybridity—zones where agricultural production, residential housing, and industrial activities coexist in complex patterns. Around Urmia, rurban spaces have proliferated, reflecting dispersed, fragmented, and uncoordinated development. Clarifying this conceptual distinction is essential for situating the Iranian case within broader comparative debates on landscape urbanism and urban ecology.

Methodologically, scholars have employed a variety of approaches to examine urban expansion. Predictive models such as Cellular Automata–Markov simulations and SLEUTH have been widely used in metropolitan contexts to anticipate future land-use change (Mirzakhani et al., 2025). While powerful, these models require extensive socio-economic datasets and calibration parameters that are often unavailable in medium-sized cities. Consequently, descriptive approaches that integrate spatial indices and landscape metrics provide a pragmatic yet rigorous framework for analyzing growth in data-limited settings. This study follows such an approach, combining three expansion indicators—the Average Annual Urban Expansion Rate (AUER), Urban Expansion Intensity Index (UEII), and Urban Expansion Differentiation Index (UEDII)—with spatial metrics including Aggregation Index (AI), Mean Radius of Gyration (MRoG), and Euclidean Nearest Neighbor (ENN). Additionally, Geographically Weighted Regression (GWR) is employed to capture spatially varying relationships between expansion intensity and landscape patterns.

By focusing on Urmia, this study makes both empirical and theoretical contributions. Empirically, it documents how urban expansion

in a medium-sized Iranian city has unfolded over three decades, highlighting its fragmented and dispersed nature. Theoretically, it situates these findings within global debates on urban growth, showing how secondary cities reflect but also diverge from patterns observed in megacities. Linking the Urmia case to international discourses on sprawl, compact city strategies, and the Sustainable Development Goals strengthens the relevance of the findings for both local and global audiences.

Accordingly, this study addresses the following three research questions:

1. How has urban expansion in Urmia evolved spatially and temporally between 1990 and 2020?
2. What are the dominant patterns of landscape change—particularly aggregation, compactness, and isolation—associated with this expansion?
3. How do urban expansion intensity and differentiation indices relate to spatial metrics as revealed by geographically weighted regression (GWR)?

By answering these questions, the study contributes to a deeper understanding of how medium-sized cities in developing contexts experience urban sprawl. The findings offer practical insights for designing infill development strategies, integrated land management, and sustainable growth pathways in data-scarce environments, thereby aligning local planning practices with global sustainability and climate resilience agendas.

MATERIALS AND METHODS

Study Section

Urbanization refers to the migration of populations from rural to urban areas. Iran is rapidly urbanizing; by 2023, over 76% of its population resides in urban areas, compared to only 51% in 1986. The nation's population has

steadily grown over the past five decades and is expected to continue this trend.

Urmia, the capital of West Azerbaijan province, lies adjacent to Lake Urmia and covers about 11,230 hectares. The city slopes from west to east toward the Urmia plain. According to the 2015 census, its population was 736,224, ranking it the second most populated city in northwest Iran and the tenth in the country overall.

Land Cover mapping

Landsat satellite imagery from 1990, 2000, 2010, and 2020 was used to generate land cover maps. Land cover classes in Urmia were categorized into four groups: built-up areas, vegetation (forest and non-forest), water bodies, and barren lands. All classification procedures were performed in the Google Earth Engine platform using an image-averaging approach to minimize atmospheric noise and ensure geometric and radiometric consistency. Composite images were generated for each decade by averaging a collection of cloud-free summer-season scenes.

Although image averaging improves data quality, it may introduce minor phenological bias due to seasonal vegetation variations. All data were taken from the LANDSAT/LC08/C01/T_SR collection, which includes geometrically and atmospherically corrected surface reflectance products.

Three indices—UI, SAVI, and MNDWI—were chosen to represent land cover based on the primary components of land cover. In this study, SAVI was used because of its advantage over NDVI to highlight vegetation features. The choice of SAVI was particularly appropriate for the semi-arid conditions of Urmia, where soil brightness strongly affects vegetation reflectance. For urban detection, the Urban Index (UI) was applied instead of the more commonly used NDBI. A comparative assessment confirmed that UI yielded higher classification accuracy for Urmia. Similarly, MNDWI was selected for water

detection because of its superior performance in identifying shallow water features compared to NDWI.

An indicator of vegetation cover that is measured and tracked using remote sensing is the Soil Adjusted Vegetation Index (SAVI). For measuring and tracking vegetation, the SAVI index is an effective tool. Vegetation mapping, vegetation health monitoring, land use classification, and crop yield calculation are just a few of the GIS applications that use it (Huete, 1988; Qi et al., 1994; Jensen, 2016; Tucker et al., 1985). The vegetation index values in areas with sparse vegetation and exposed soil surfaces may be impacted by the reflectance of red and near-infrared wavelengths (Huete, 1988). According to Jensen (2005) and Li et al. (2016), SAVI makes use of the significant pigment absorption of red light, such as the TM 3 band, and the NIR spectral range, such as the TM 4 band, which has high vegetative reflectance. Due to SAVI's superior ability to analyse regions with little vegetation, including urban areas, and emphasize vegetation traits, we choose to utilize it instead of the normalized difference index (NDVI). SAVI is applicable to regions with a minimum of 15% plant cover. But in places where there is at least 30% plant cover, NDVI can be applied successfully (Herold et al., 2015). Equation 1 shows the soil-adjusted vegetation index (SAVI), where NIR is the near-infrared sensor's reflectance value (TM band 4). The color red in the TM sensor indicates the reflectance value of band 3 (red). L is a correction factor that has values of 1 for extremely low density and 0 for very high density. An enhanced vegetation image was produced, taking into account the medium density of vegetation in the analyzed area. By increasing its range, SAVI may differentiate between built-up or dry land and vegetation using a value of 0.5. Vegetation, therefore, exhibits strong reflection in the near-infrared range and low reflectance in the red band; this is the basis of SAVI. In order to reduce the impact of soil

illumination on the SAVI value, the soil illumination correction factor is applied (Huete et al., 1991; Zhang et al., 2003).

Equation 1:

$$SAVI = [(NIR - Red) / (NIR + Red + L)] * (1 + L)$$

L is a correction factor, and it goes from very low densities (value = 1) to very high densities (value = 0). For this reason, SAVI is superior to other vegetation indices, like the Normalized Difference Vegetation Index (NDVI), in many ways. Firstly, compared to NDVI, SAVI is less susceptible to soil brightness. Second, according to Huete (1988), Qi et al. (1994), and Jensen (2016), SAVI is more successful in differentiating between plants and other types of land cover, such as soil and water. Equation 2 was used to build the constructed terrain image using Urban Index (UI), following the generation of the vegetation image using SAVI. The sensor measures band 4 (near infrared) and band 7 reflectance values, which are referred to as NIR and SWIR. An effective technique for locating and keeping an eye on urban areas is the UI index. Urban area mapping, urban growth monitoring, urban land use classification, and urban heat island monitoring are just a few of the GIS applications that employ it (Zha et al., 2003; Kawamura et al., 1992; Huang et al., 2019; He et al., 2015).

Equation 2:

$$UI = SWIR - NIR / SWIR + NIR$$

Where:

UI is an urban index.

SWIR represents reflectance values in the shortwave infrared (SWIR) band commonly found in remote sensing data.

NIR indicates reflectance values in the near-infrared (NIR) band.

The idea behind the urban index (UI) is that urban areas have relatively high reflectance in the SWIR band due to materials commonly found in cities, such as concrete and asphalt. In contrast, natural or non-urban areas typically have lower SWIR reflectance. By calculating UI, it is

possible to create an index that increases the spectral differences between land cover types and makes it easier to distinguish between urban and non-urban areas.

In order to aid in distinguishing between populated areas and wasteland, the urban index (UI) was employed. The Normalized Difference Making Index (NDBI) is less recognizable than the Urban Index (UI) in terms of urban characteristics. Band 7 yields the best results when band 5 is not employed (Bouhennache et al., 2015; Pratibha et al., 2014). Consequently, these urban index values were used instead of the Normalized Difference Making Index (NDBI) data. In general, increasing the range of SAVI can differentiate vegetation from built-up land or wasteland. In summary, the urban index (UI) has many advantages over other urban indices, such as the normalized difference index (NDBI). First, the user interface is less sensitive to atmospheric interference than NDBI. Second, UI is more effective in distinguishing between urban areas and other types of land cover, such as soil and vegetation.

A background primarily made up of developed land is distinguished from water using the modified normalized water change index (MNDWI). Zhou (2005) claims that, in terms of outcomes, MNDWI has done better than the normal water difference index (NDWI). The modified NDWI (MNDWI), where the MIR is a mid-infrared band similar to the 5 TM band, is described by equation 3 (McFeeters, 1996). Due to an increase in the values of water features and a drop in the values of built-up land, the MNDWI's contrast between water and built-up land will drastically change from positive to negative when compared to the NDWI (Hu, 2007).

Equation 3:

$$MNDWI = (Green - SWIR) / (Green + SWIR)$$

Where:

MNDWI: Normalized water change index.

Green: Indicates the reflectance values in the green spectral band.

SWIR: Shows reflectance values in the short-wave infrared (SWIR) band.

To enhance its sensitivity to shallow water and decrease false positives in water detection, Zhou (2006) modified the normalized water difference index (NDWI) and introduced MNDWI. The foundation of MNDWI is the idea that water has low reflection in the mid-infrared band and high reflectivity in the green band. The reason for this is that green light is reflected to the satellite sensor and is absorbed by water in the mid-infrared spectrum. Compared to other water indices, including the Normalized Difference Water Index (NDWI), MNDWI has a number of advantages. First, MNDWI is less sensitive to atmospheric interference than NDWI. Second, MNDWI is more effective in distinguishing between water and other land cover types, such as soil and vegetation. This index has been widely used in applications related to water resources management, wetland mapping, and flood monitoring due to its effectiveness in highlighting the features of open water (Hu, 2006; McFeeters, 1996; Feyisa et al., 2014; Gao et al., 2009; Zhang et al., 2018).

Following the creation of the SAVI, MNDWI, and UI pictures, three new photos were used as the bands in a new dataset. The correlation between the bands is significantly reduced when the thematic three-band image is substituted for the original seven-band multispectral image. Then, a fresh image was produced by combining three more bands.

The supervised classification procedure was carried out using a support vector machine technique. Consequently, Figure 1 illustrates how the four primary types of urban land cover are effectively divided: vegetation (high SAVI value), water (high MNDWI values), built-up area (high UI value), and barren land (low UI value). To evaluate the reliability of classification, an accuracy assessment was

conducted using confusion matrices and kappa statistics. Ground-truth samples were collected from high-resolution Google Earth imagery. Overall classification accuracy ranged from 86% to 89%, with kappa coefficients between 0.82 and 0.88, indicating strong agreement and validating the classified maps. A limitation of this approach is the exclusive reliance on Landsat data. Although adequate for long-term analysis, higher-resolution datasets such as Sentinel or socio-economic data could provide complementary insights, which remain beyond the scope of this study.

Gradient Model

The gradient model effectively represents spatiotemporal transitions between urban and rural areas (McDonnell & Pickett, 1990; Zhang et al., 2016; Cheng et al., 2019; Yang et al., 2022). In this study, it was used to analyze Urmia's expansion across both space and time by integrating remote sensing and GIS-based buffer analysis.

The Central Business District (CBD) was defined as the urban core, surrounded by 20 concentric buffer zones (each 1 km wide) covering the entire city. These zones were then divided into eight directional sectors—N, NE, E, SE, S, SW, W, NW—to extract and compare built-up area data directionally. This approach allows the identification of asymmetric growth patterns and the detection of directional preferences in expansion.

While this model offers a simplified yet practical spatial framework, it assumes a monocentric city form. However, Urmia—like many medium-sized Iranian cities—has evolved multiple sub-centers in recent decades. This polycentric reality can bias the gradient analysis, particularly in peripheral districts where secondary nodes influence land-use transitions. Accordingly, this methodological limitation was acknowledged when interpreting results.

Figure 2 illustrates the spatial delineation of built-up zones and urban expansion in Urmia between 1990 and 2020.

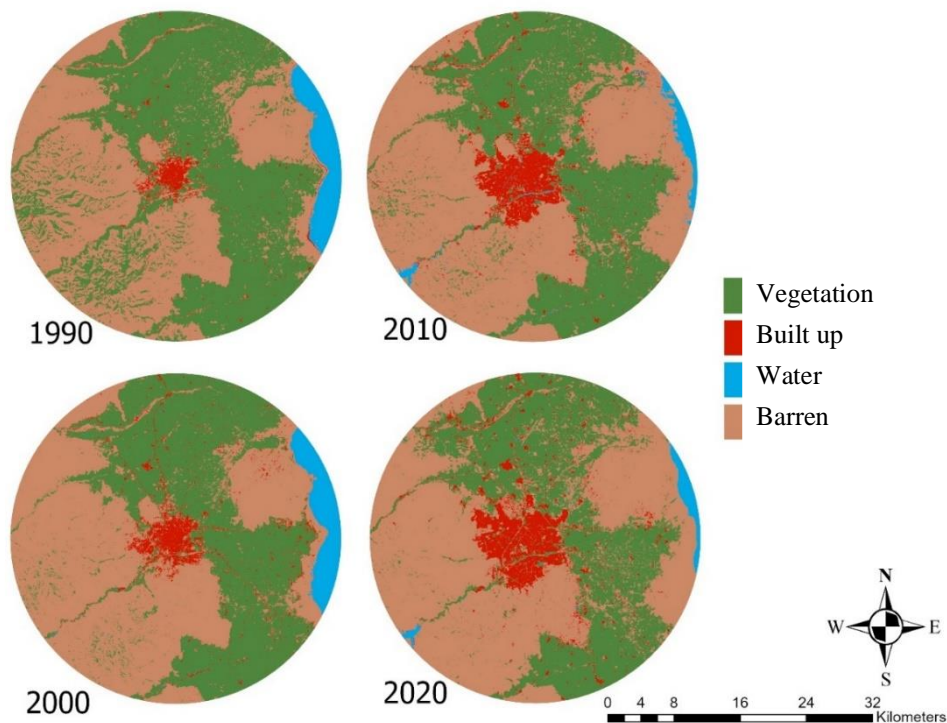


Fig 1. Classified Images of Urmia Urban Area (1990-2020)

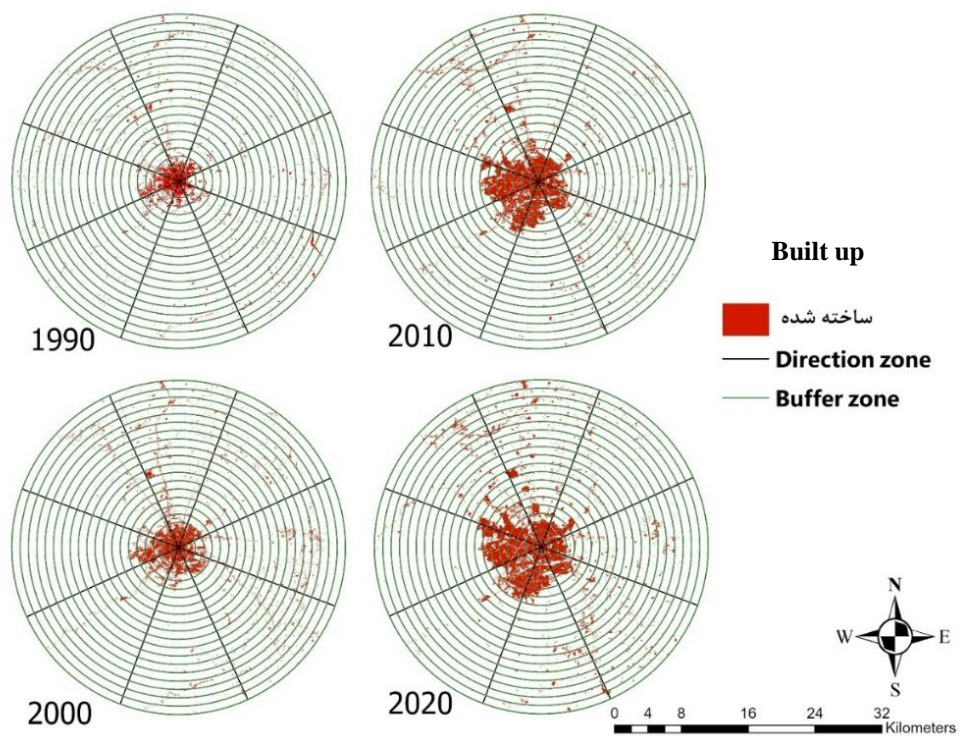


Fig 2. Built-up Lands and Zoning of the Urmia Urban Area in the Period of 1990-2020

Urban Expansion Measurement

The pace, volume, and intensity of urban expansion have all been studied, and growth ratio indicators and geographic information system (GIS) analytical techniques have been used in several of these investigations. Urban expansion intensity index (UEII) (Hu et al., 2007; Herold et al., 2015), landscape expansion index (LEI) (Liu et al., 2009), and urban expansion differentiation index (UEDI) are a few examples. Certain ones have been utilized on a frequent basis. Urban expansion was measured in this study using a mixed method (Heidarinejad, 2017).

The first statistical index to determine the average annual urban growth rate is the Average Annual Urban Growth Rate (AUER) (Equation 4). According to Acheampong et al. (2016), this indicator determines the built-up land's average yearly increase during the course of the study period in a case study. Although it can be computed for any duration, AUER is typically computed for yearly intervals. An effective metric for comprehending and controlling urban growth is AUER. It can be used to monitor the rate at which urban areas are growing, pinpoint regions that are seeing fast urbanization, and evaluate how urban development affects other forms of land cover (Seto et al., 2012; Angel et al., 2007; Zhao et al., 2020).

Equation 4:

$$AUER_i = \left[\left(\frac{ULA_{it2}}{ULA_{it1}} \right)^{\frac{1}{\Delta t}} - 1 \right] \times 100$$

where AUER_i is the annual urban expansion rate. ULA_{it2} and ULA_{it1} are the areas of unit *i* at times *t2* and *t1*, respectively. AUER is not affected by the size of the spatial unit. Δt is the study period.

Furthermore, this study has employed the Urban Expansion Intensity Index (UEII).

Equation 5 illustrates how the UEII determines a geographical unit's annual average proportion of

newly built-up land, standardised by the unit's total area (Manesha et al., 2021). The following is its formula (Li et al., 2015).

Equation 5:

$$UEII_i = \frac{|ULA_{it2} - ULA_{it1}|}{TLA_i \times \Delta t} \times 100$$

Unit *I*'s urban expansion intensity index is denoted by UEII_i, whereas ULA_{it2} and ULA_{it1} represent the areas within unit *I* at periods *t2* and *t1*, respectively. The entire area in unit *I*, *t* of the research period is denoted by TLA_i. Consequently, the computation involves splitting the mean yearly rate of urban growth by the entire area of a certain geographic region. Higher values of the unitless UEII index denote a faster and more intensive rate of urban expansion (MacGregor-Fos et al., 2022; Liu et al., 2021; Zhou et al., 2020).

Changes in the amount of urban area per unit of time can be assessed using the urban growth intensity index. This index is important for assessing the geographical variations of urban growth because it provides a quantitative assessment of the volume and intensity of urban expansion (Heidarinejad, 2017; Medayese et al., 2023). Urban expansion will vary depending on the regulation of urban driving variables and their geographical consequences during the expansion process.

The preference for urban growth is the term used to describe this tendency (Alsharif and Pradhan, 2013; Heidarinejad, 2017). Urban spatial expansion has been quantitatively evaluated and analyzed in this study using UEII. Furthermore, the desire for urban expansion during a given time period was identified using UEII. UEII measures the intensity of changes in urban cover over time and represents potential for urban expansion. The Urban Expansion Intensity Index (UEII) scores of the 20 concentric regions that comprise the region are divided into five UEII regions (Table 1) to reflect the spatial

evolution pattern of urban land growth (Heidarinejad, 2017; Alsharif et al., 2015).

Furthermore, the Urban Expansion Differentiation Index (UEDI) determines the proportion of the total altered area to the growth in the urban area of one unit (proportionally). In contrast to UEII, UEDI measures the difference in urban land expansion between various spatial units. It so renders the units comparable (Acheampong et al., 2016; Heidarinejad). The differentiation or diversity in urban growth patterns in a given area is assessed and quantified using the urban expansion differentiation index (UEDI), which is used in land use analysis and urban planning. This index offers insightful information about the nature and spatial distribution of urban growth throughout time (Zhao et al., 2020; Yan et al., 2018). This criterion is useful in evaluating the differentiation of urban land expansion and identifying hot spots of urban expansion. The formula for this case is as follows (Li et al., 2015):

Equation 6:

$$UEDI_i = \frac{|ULA_{it2} - ULA_{it1}| \times ULA_{it1}}{|ULA_{it2} - ULA_{it1}| \times ULA_{it1}} \times 100$$

The entire area of unit *i* at times *t2* and *t1*, respectively, is represented by *ULA_{it1}* and

ULA_{it2}, while the differentiation index of urban expansion in unit *i* is denoted by *UEDI_i*. Generally speaking, UEDI can be divided into three categories: (1) The study region as a whole classifies a region as fast-growing when the differentiation index of the constituent geographical unit, or region, is greater than 1; (2) When the region differentiation index equals 1, the region is compared to the region; and (3) when the region differentiation index is less than 1, in which case the region is defined as a slow-growth region in respect to the case study, and Table 2 categorizes the research area as a medium growth area (Acheampong et al., 2016; Heidarinejad, 2017).

The integration of AUER, UEII, and UEDI forms a robust descriptive framework for spatiotemporal assessment of urbanization. While predictive models such as CA–Markov, SLEUTH, and CLUE-S (Mirzakhani et al., 2025) provide forward simulations, they demand detailed socio-economic datasets that are often unavailable for medium-sized cities like Urmia. Thus, these indices offer a data-efficient alternative, effectively capturing the ecological and structural logic of past growth and supporting urban management in data-limited contexts.

Table 1. Range of Urban Expansion Intensity Index

Range	Potentials of Urban Expansions
$0 < UEII \leq 0.28$	Slower development
$0.28 < UEII \leq 0.59$	Low-speed development
$0.59 < UEII \leq 1.05$	Medium-speed development
$1.05 < UEII \leq 1.92$	High-speed development
$UEII > 1.92$	Extremely high-speed development

Ref: Acheampong et al. (2016); Heidarinejad (2017)

Table 2. Range of the Differentiation Index for Urban Expansion

Range	Urban Expansion Differentiation
$UDEI > 1$	Fast-Growing Area
$UDEI = 1$	Moderate Growing Area
$UDEI < 1$	Slow-Growing Area

Ref: Acheampong et al. (2016); Heidarinejad (2017)

Measurement of Urban Spatial Patterns

Spatial metrics provide quantitative descriptions of the spatial arrangement of land-use features, capturing their size, form, and connectivity. To examine Urmia's urban expansion, three key dimensions of spatial configuration were analyzed using Fragstats 4.2 (McGarigal et al., 2012). These include aggregation (AI), compactness (MRoG), and connectivity (ENN_MN). Although numerous metrics exist, many are highly intercorrelated (McGarigal et al., 2012). Therefore, we selected a concise set representing complementary aspects of spatial structure.

Quantifying the spatial patterns' accumulation level is a crucial step in urban pattern analysis (Hong et al., 2000; Clark & Evans, 1954). He et al. (2001) claim that the aggregation index is a useful tool for managing and understanding spatial patterns in the surrounding environment. The aggregation index (AI) is a spatial statistic that quantifies the degree to which related characteristics are aggregated or clustered together in a landscape or spatial dataset.

The aggregation index is the number of adjacencies of a given land cover class divided by the maximum number of adjacencies that may potentially belong to that class. It may be more effective since it allows one to concentrate on just one class at a time (Alberti, 2008). This index indicates the degree to which the objects in a given region are distributed or grouped. Evaluating the spatial distribution of species or phenomena is helpful in a number of fields, such as ecology, geography, and urban planning. Because this index is class-specific, it is more accurate than other indices that measure landscape aggregation generally. Consequently, AI provides a quantitative basis for linking a class's spatial pattern to a specific process. The map units have no bearing on the computation because the aggregate index is a ratio variable. It may be contrasted with other or comparable

picture classes, or even with other similar classes of the same image at various resolutions (Hong et al., 2000; Heidarinejad, 2017). The specific formula and method for calculating the aggregation index can differ depending on the research question, the type of data, and the software used. These methods consider the spatial arrangement of features and compare them to a random or uniform distribution to determine whether the features are clustered or scattered. In the context of urban expansion, an increase in AI may have two interpretations. On one hand, higher AI can indicate compact growth, which is desirable for sustainable urban form and infrastructure efficiency. On the other hand, if unregulated, higher AI may reflect overcrowding or the concentration of development without adequate services. This duality is important for interpreting results in policy terms.

Compaction indices are calculated to determine the urban footprint. The urban footprint is almost a circle. This study uses the mean radius of gyration (MRoG) as a convenient tool to measure the extent of patches and joints, which preserves the actual measurement units (meters). The mean radius of gyration is a spatial metric that measures the dispersion of habitat patches around a central point. Thus, the average gyration index provides insights into how objects are concentrated or dispersed in a region. The average radius of the gyration index is equal to the average distance (m) between each cell in the patch and the center of the patch (Heidarinejad, 2017; Botequilha et al., 2006; Baker et al., 2015; Rocha et al., 2016). As a result, the mean radius of rotation is a useful measure to evaluate the impact of land use change on landscapes (Baker et al., 2015). A smaller mean radius of gyration (MRoG) index indicates compactness, while a larger mean radius of gyration (MRoG) index indicates that objects are more scattered from their center (Wang et al., 2018; Pérez-Hernández et al., 2018). It should be noted that the Mean Radius of Rotation Index (MRoG) is a powerful

tool for understanding and managing the terrain. It is a relatively new measure, but it has quickly gained popularity among climate ecologists and researchers from other disciplines (McGarigal et al., 2012; Rocha et al., 2016). While MRoG has been less commonly applied in urban studies, its novelty lies in capturing both the dispersion and compaction dynamics of urban patches. This metric highlights whether new development is reinforcing a compact urban core or dispersing into peripheral rurban areas, making it particularly relevant for medium-sized cities experiencing fragmented sprawl.

An effective spatial measure for determining the average distance between items or points in a collection is the Euclidean Mean Nearest Neighbor (ENN_MN). In spatial analysis, knowing the general spatial distribution of features or objects is very useful. This measure sheds light on whether items in a study area scatter or cluster. Therefore, a spatial statistic that calculates the average distance between a point and its nearest neighbor in the same class is called the average Euclidean distance of the nearest neighbor. It is computed by dividing the total number of points by the sum of the distances between each point and its closest neighbors within a class. According to the shortest straight-line distance determined from the cell centers, Euclidean Mean Nearest Neighbor (ENN_MN) determines the distance to the closest neighboring patch of the same kind (McGarigal and Marks, 1995; Diggle, 2013; Jin & He, 2012; Liu et al., 2019). Euclidean nearest neighbor mean values are never less than zero and never have boundaries. This index gets closer to 0 as the distance from the closest neighbor gets smaller. The cell size, which is equal to twice the cell size when applying the neighboring patch rule, sets a minimum value for this index. The size of the territory, which in this study is the size of the block, sets an upper limit. The average Euclidean nearest neighbor is not defined if the patch has no neighbors, that is, no other patches of the same

class (Heidarinejad, 2017; McGarigal, 2012). As a result, the index's value represents the typical separation between an object and its closest neighbors. A smaller value denotes clustering or spatial dependence, meaning that objects are more likely to be found in close proximity to their immediate neighbors. Conversely, a greater value suggests that the items are dispersed more widely or uniformly within the research region (Diggle, 2013; Jin & He, 2012). ENN_MN provides critical insights into connectivity and accessibility. Lower ENN values suggest clustered development, which may enhance service delivery and transport efficiency, while higher ENN values indicate fragmented, isolated growth. This has direct implications for planning pedestrian and transport networks, as increased isolation at the periphery can exacerbate socio-spatial inequalities.

Regression

To explore how urban expansion influences spatial patterns, variations in spatial metrics were modeled against urban growth indices. The dependent variables included changes in AI, MRoG, and ENN_MN, while the independent variables were the Urban Expansion Intensity Index (UEII) and Urban Expansion Differentiation Index (UEDI). Among regression approaches, Geographically Weighted Regression (GWR) was adopted for its ability to capture spatially varying relationships between variables (Heidarinejad, 2017; Fotheringham et al., 2002). Unlike global regression, which assumes constant coefficients, GWR estimates a local equation for each spatial unit, providing geographically adaptive coefficients that reveal regional disparities. Prior to modeling, diagnostic tests confirmed the absence of multicollinearity and significant spatial autocorrelation in residuals. The kernel bandwidth was optimized using the Akaike Information Criterion (AIC) to balance model fit and spatial smoothness. This

regression's equation (Equation 7) can be written as follows (Zhou et al., 2020; Fotheringham et al., 2002).

Equation 7:

$$\hat{y}_i = \beta_0(u_i v_i) + \sum_k \beta_k(u_i v_i) x_{ik} + \varepsilon_i$$

Where \hat{y}_i is the estimated value of the dependent variable for observation i , β_0 is the cross-sectional variable, β_k is the parameter estimate for variable k , x_{ik} is the value of the k th variable for i , ε_i is the error term, and $(u_i v_i)$ takes the coordinate location of i .

It is posited that the influence of nearby observations on each other's parameter estimation is more than that of distant observations. A distance decay function with observation i at its center determines the weight given to each observation. The distance between polygon centers is used to compute the distance between observations when dealing with regional data. Where the weight distance quickly approaches zero, a bandwidth adjustment modifies the distance decay function, which might take on many shapes. The analyst might choose the bandwidth manually or by optimizing it with an algorithm that aims to reduce the cross-validation (CV) score. As an alternative, the Akaike Information Criterion (AIC) score can be minimized to determine the bandwidth (Equation 8) (Medayese et al., 2023; Heidarinejad, 2017; Nakaya et al., 2005).

Equation 8:

$$AIC_t = 2n \log_e(\hat{\sigma}) + n \log_e(2\pi) + n \left\{ \frac{n + \text{tr}(S)}{n - 2 - \text{tr}(S)} \right\}$$

One benefit of using the AIC technique is that it accounts for the possibility of multiple degrees of freedom in models based on different observations. Furthermore, the user can select between a variable bandwidth that grows and decreases in the model over regions with sparse observations, or a fixed bandwidth that is used for

each observation. Regressing regions of dense observations is more crucial for the model with a lower AICt value. For the GWR model, the AICt approach was therefore applied in this investigation (Medayese et al., 2023; Heidarinejad, 2017; Griffith, 2008).

RESULTS AND DISCUSSION

In this research, the appearance of land use changes in a specific area in four different decades (1990, 2000, 2010, and 2020) is very important. These data are obtained from remote sensing images and image processing techniques, and make it possible to interpret changes in urban expansion, vegetation, water resources, and land cover status of the region.

These observed land cover changes are not only physical but also socially driven, reflecting rural–urban migration, industrial policy shifts, and weak enforcement of land-use regulation.

According to the data in Table 3 and Figure 3, in 1990, the total area of the study area was equal to 1254.80 square kilometers. 47.71% (598.67 square kilometers) belonged to vegetation. This percentage gradually decreased in the following years and decreased to 35.83% in 2020. This decrease represents the increase in construction activities and urban development, which, on the one hand, requires urban development and, on the other hand, affects the issues related to the preservation of natural resources and vegetation. Beyond physical land cover change, these dynamics reflect broader socio-economic drivers. Rapid migration from surrounding rural areas, coupled with weak land-use regulation, has accelerated the conversion of agricultural lands. Industrial policies and the expansion of service activities in Urmia have further attracted population inflows, reinforcing urban growth pressures.

Table 3. Area and Share of Land Use

Year	1990		2000		2010		2020	
Land use	Km ²	%	Km ²	%	Km ²	%	Km ²	%
Vegetation	598.67	47.71	505.70	40.30	482.44	38.45	449.56	35.83
Built-Up	34.43	2.74	63.13	5.03	87.33	6.96	109.64	8.74
Water	56.94	4.54	56.46	4.50	24.04	1.92	17.80	1.42
Barren-Land	564.76	45.01	629.50	50.17	660.98	52.68	677.78	54.02

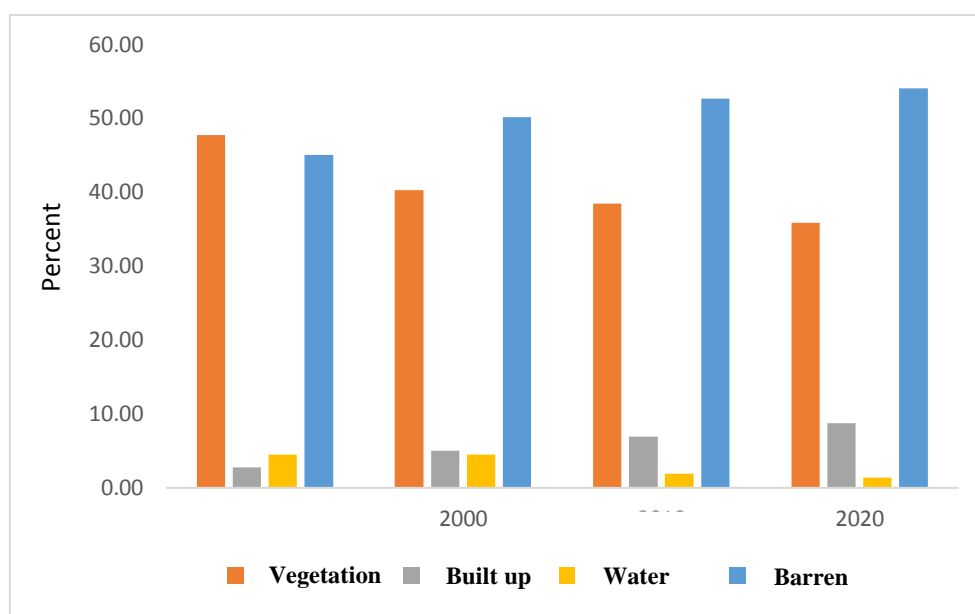


Fig 3. Share of Land Uses (1990-2020)

The share of built-up users has also increased greatly in these periods. In 1990, only 2.74% (34.43 km²) of the area was built-up. But, in 2020, this number had increased to 8.74% (109.64 square kilometers). This increase represents comprehensive urban development and changes in the urban structure of the region.

As for surface waters, their area in 1990 was equal to 4.54% (56.94 square kilometers) of the total area and has shown a continuous decrease in the following years. In 2020, only 1.42 percent (17.80 km²) of the area was devoted to water. This decrease represents the lack of water resources and changes in the region. This issue raises the need for proper management of water resources. These changes are also symptomatic of broader environmental stress. The desiccation of Lake Urmia, linked to both climate variability and unsustainable water extraction, has intensified barren land expansion. Situating the findings

within climate change debates underscores how urban growth in Urmia compounds existing ecological vulnerabilities.

Barren lands have also played an important role in these changes. Their area has increased from 45.01 percent (564.76 square kilometers) in 1990 to 54.02 percent (677.78 square kilometers) in 2020. This increase represents the changes in the geological and climatic conditions of the region.

In general, a detailed analysis of these data shows that several factors have influenced land use changes during these four decades. The increase in the built surface and the decrease in plants in cities represent the processes of urbanization and urban development. Instead, the reduction of water resources and the increase of barren lands represent changes in the geological and climatic conditions of the region.

Table 4. Conversion between Land Uses (KM2)

Period			
Class	1990-2000	2000-2010	2010-2020
1->2	21.73	10.95	16.59
1->3	1.39	1.59	0.29
1->4	103.54	56.43	57.84
Total	126.66	68.98	74.72
2->1	4.00	11.73	5.65
2->3	0.14	1.51	0.09
2->4	8.35	8.85	14.18
Total	12.49	22.08	19.92
3->1	0.03	1.07	2.11
3->2	0.20	0.62	0.48
3->4	2.45	36.82	5.43
Total	2.68	38.52	8.03
4->1	29.73	32.93	34.06
4->2	19.29	34.70	25.16
4->3	0.68	2.93	1.39
Total	49.70	70.56	60.61

1- Vegetation 2- Built-up 3-Water 4- Barren

In Table 4, land use transformations in different time frames for four land classes (vegetation, built-up, water areas, and barren) are given in the study area. This table shows the changes that have occurred in land use during the specified period of time.

Between 1990 and 2000, 21.73 square kilometers of vegetation land (land class 1) were converted into built-up areas (land class 2). This value decreased to 10.95 square kilometers in the next decade. But in 2010-2020, there was an increasing trend, and vegetation conversion to built-up area was 16.59 square kilometers. Similar transformations are observed in land class 1 (vegetation) to land class 3 (water areas). These changes show that several vegetated lands have turned into water areas. But these changes have decreased in recent decades compared to previous decades. Also, a similar trend is observed in converting vegetation to barren. So, in 1990-2000, the conversion rate was 103.54 square kilometers. But in the following decades, it has decreased to 56.43 and 57.84 square kilometers.

In general, reducing vegetation and converting it to other uses, especially barren and built lands, is evident in all decades. In the last decade, this conversion has increased. Another significant trend related to converting irrigated lands to barren lands, especially in 2000-2010, is that about 36.82 square kilometers of irrigated areas have been turned into barren lands. The conversion of barren land into built-up land is also a good indication of the result of urban expansion in the urban area of Urmia, the highest amount of which was 34.70 square kilometers in the years 2000-2010.

In 1990, the built area was 34.43 square kilometers, which increased over the years and reached 109.64 square kilometers in 2020. Therefore, the share of built area has also increased in these periods. In 1990, the built-up area of the total area was 2.74%, and in 2020 it increased to 8.74%. This increase in the share of the built area shows urban growth and urban development in these periods. Furthermore, the annualized growth rate (AUER) shows that

approximately 83.3% of this increase occurred in the initial period. Compared to 25.5% in the last 10-year period, the volume of urban expansion in the first period was the highest (Figure 4).

Overall, the analysis shows that the city expanded continuously during these periods. The built area has increased in proportion to the total area. It may indicate urban expansion and population growth.

Evolutionary-temporal Features of Urban Land Expansion

Every place and direction may experience urbanization in a different way. This phenomenon is indicative of the urban area's growth. The Urban Expansion Intensity Index (UEII) adjusts the yearly rate of urban growth for every study unit based on its land area. This score was utilized in the current study to determine if urban expansion was preferred over a 30-year period in a case study. The built-up area intensity in various city regions from 1990 to 2020 is contrasted in Figure 4.

Figure 5 shows that the highest values of the urban intensity index are from 1990 to 2000. This issue indicates the major occurrence of urban expansion in this period. Thus, from the city center to a distance of 4 km, it has increased rapidly to a value of 34.88, which indicates the experience of high intensity of urban expansion in this area. But the highest intensity of urban expansion occurred at a distance of 16 km with a value of 69.66. But in the following decades, the intensity of urban expansion is significant only up to a radius of 7 km, and from a distance of 8 km from the city center, with increasing distance and decreasing intensity of expansion, it has slowly decreased, and the intensity of expansion has decreased in peripheral areas. The outcome reveals that Urmia City's central regions are home to the region seeing the highest rate of expansion. However, the following decades saw a marked decline in the expansion intensity relative to the previous phase.

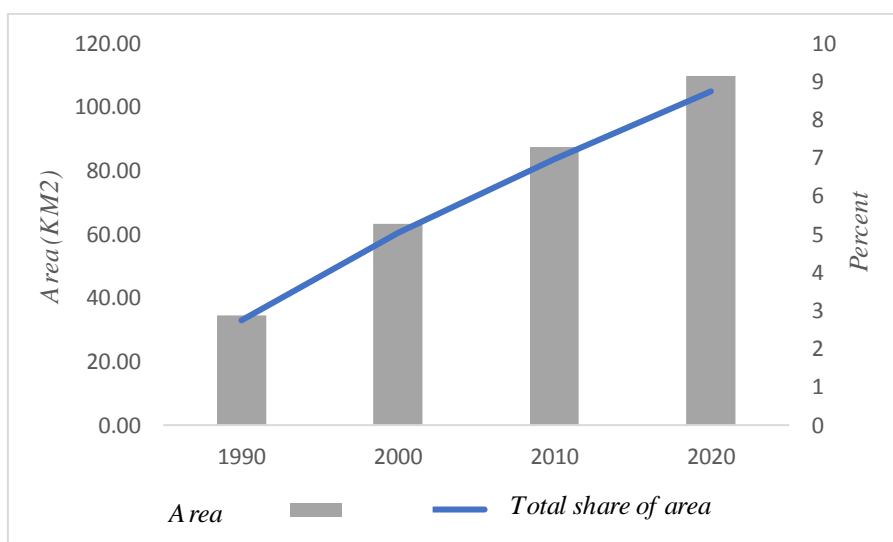


Fig 4. Area and Share of Total Built-up Land

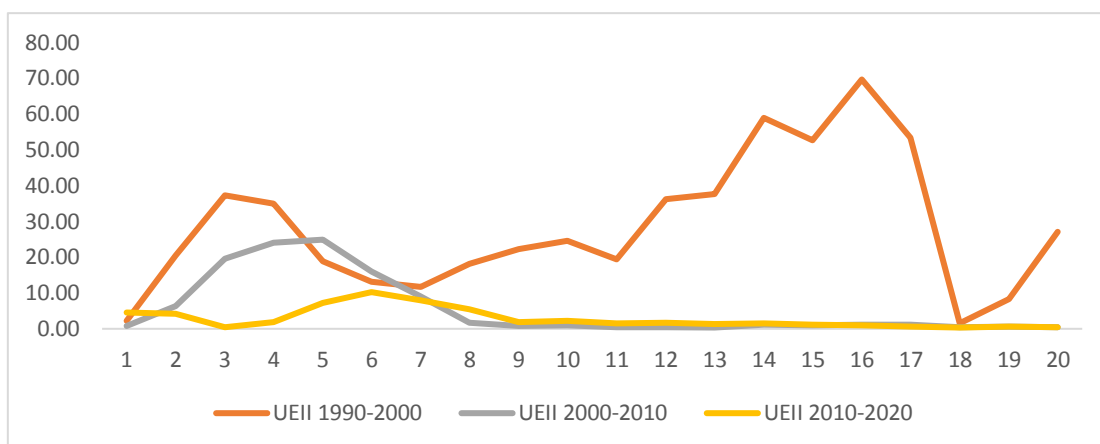


Fig 5. Changes in the Intensity Index of Urban Expansion in the Central Regions

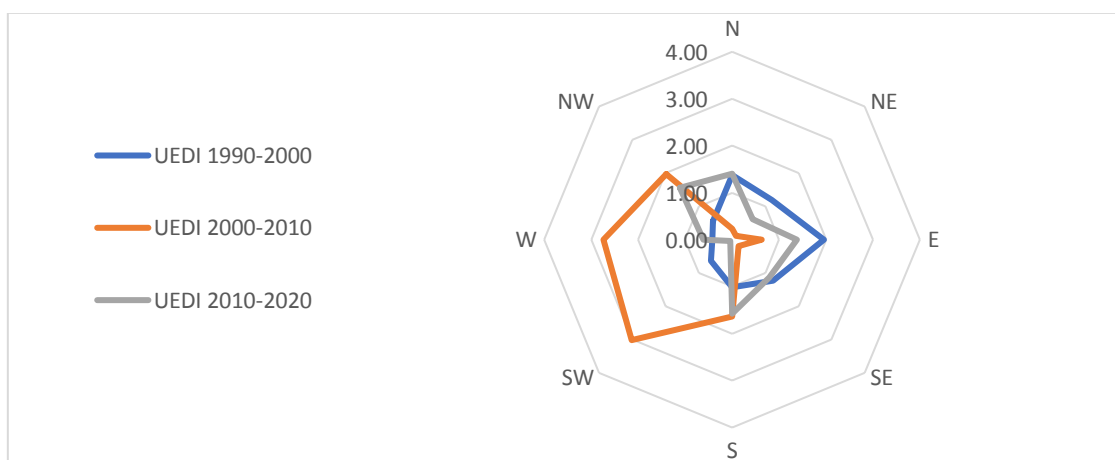


Fig 6. Urban Expansion Variations in the Intensity Index (UEII) in Different Geographical Directions

The expansion intensity index for Urmia during a 30-year period is compared in Figure 6 in various directions within the city. The primary directions of urban expansion throughout the first ten years of the 1990s–2000s were north and east. However, the rate of urban growth has accelerated in the north, west, and southwest in the ensuing decades. The tremendous rate at which the populated areas to the north of Urmia are expanding is astonishing.

The difference index, in contrast to the urban expansion intensity index (UEII), normalizes urban expansion (UEDI) to the rate of expansion throughout the metropolis, so it strengthens the uniformity between the units of spatial expansion (Achiamong et al., 2016). This indicator is frequently used to assess the trend of urban expansion and identify regions that experience significant variations in urban expansion.

It is evident from Figure 7's fluctuations in UEDI index values over a 30-year period that the model needed to be more reliable. According to the UEDI index, the beginning point in the first period was almost equal to 0 (central areas), and in the subsequent periods, it rose in the peripheral areas. The examination revealed that the case study's original center has been enlarged in subsequent years. In fact, over the past ten years, nearly all inner-city areas have increased their UEDI scores. In other words, over time, the central areas close to the previous lands are built, and as a result, urban expansion occurs at distances far from the center. Areas located within a radius of 3 to 8 kilometers from the city center have grown significantly from 1990 to 2000. The main reason is the addition of urban areas. However, the areas located in 9 to 13 km have grown less than those in 13 to 16 km, which can

be one of the reasons for establishing industries and activities related to agriculture. This illustrates how spatial heterogeneity in expansion is strongly shaped by economic policy decisions. Industrial zoning in peripheral areas and the decline of agricultural profitability in inner belts have redirected growth corridors, reinforcing fragmented sprawl rather than compact development. From 2000 to 2010, however, the largest urban expansion occurred in areas 6 and 7 kilometers from the city center, and other areas experienced even less growth compared to other decades. From 2010 to 2020, the radius of 8 km from the city center experienced the greatest expansion of built-up land. But another important thing that has happened is the significant growth of the radius of 11 to 14 kilometers of built-up

land. One of the possible reasons for this is the land use policies and the transfer of some incompatible industries and services outside the city, as well as the growth caused by the addition of rural centers to the city.

Figure 8 shows the difference index values of urban expansion in different directions. Therefore, in the first decade of 1990-2000, the greatest difference and intensity of urban expansion occurred in the direction of east and north. But, in the next decade, the desire to expand the built lands in the southwest, west, and northwest has increased. Finally, in the decades of 2010-2020, the pattern of urban expansion has tended toward the east and northern regions, which is mainly due to the increase in agricultural and industrial activities.

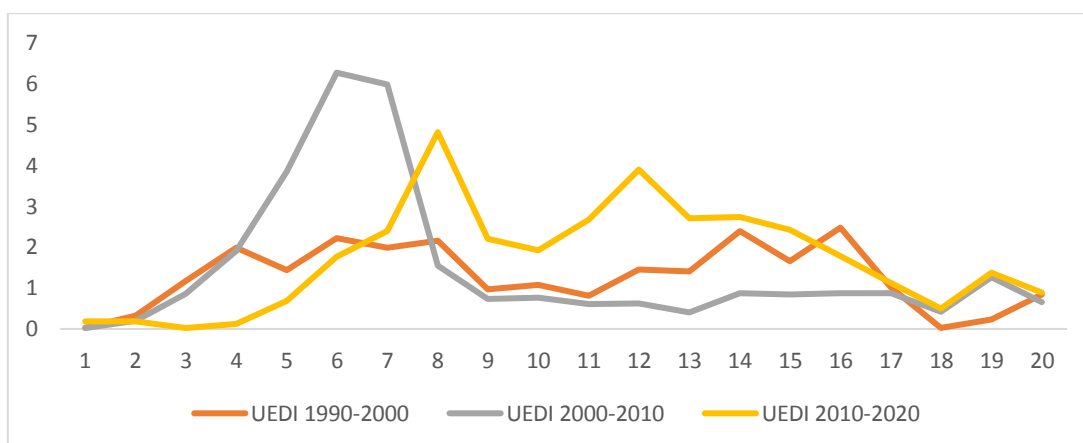


Fig 7. UEDI Index Values in Concentric Regions

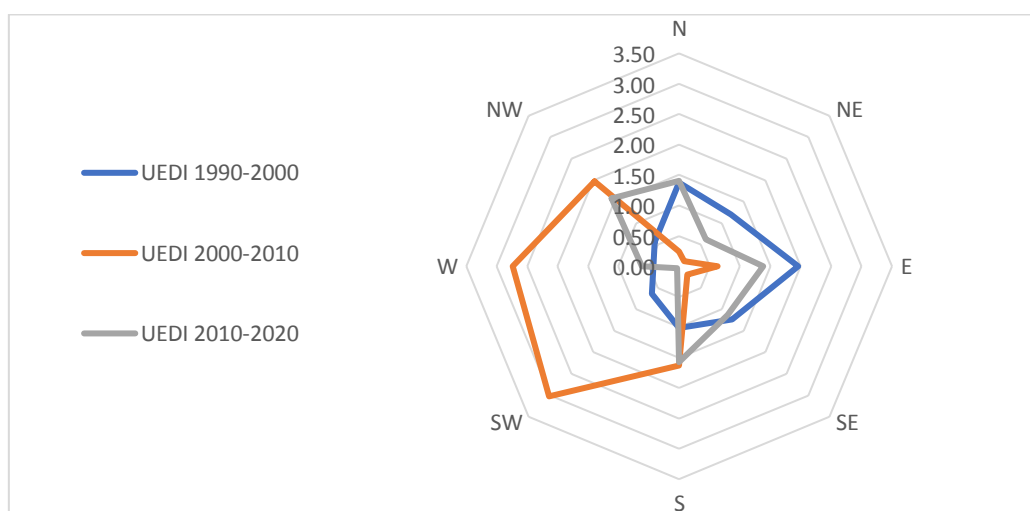


Fig 8. UEDI Index Values in Geographical Directions

In order to better understand and compare the UEDI values, the UEDI pattern in Urmia (hot spot) was examined according to three selected patterns. There are three possible expansion classes based on this index:

High (i.e. $UEDI > 1$),

Medium (i.e. $UEDI = 1$), and

Low (i.e. $UEDI < 1$) (Heidarinejad, 2017).

The top class of UEDI was split into "very high" and "high" subclasses based on the values that were obtained. Likewise, there were two categories for the lower class: "low" and "very

low". The Jenks Natural Breaks method in ArcGIS is used to display the five UEDI score classes in concentric zones in Figure 9. The spatial visualization outcomes for directional zones in this category are also displayed in Figure 10.

The acquired data indicated that during the course of two decades, marginal areas were home to the hotspots of urban expansion. The north and northeast are experiencing extremely fast expansion, whereas the west and south are experiencing the slowest rate of expansion.

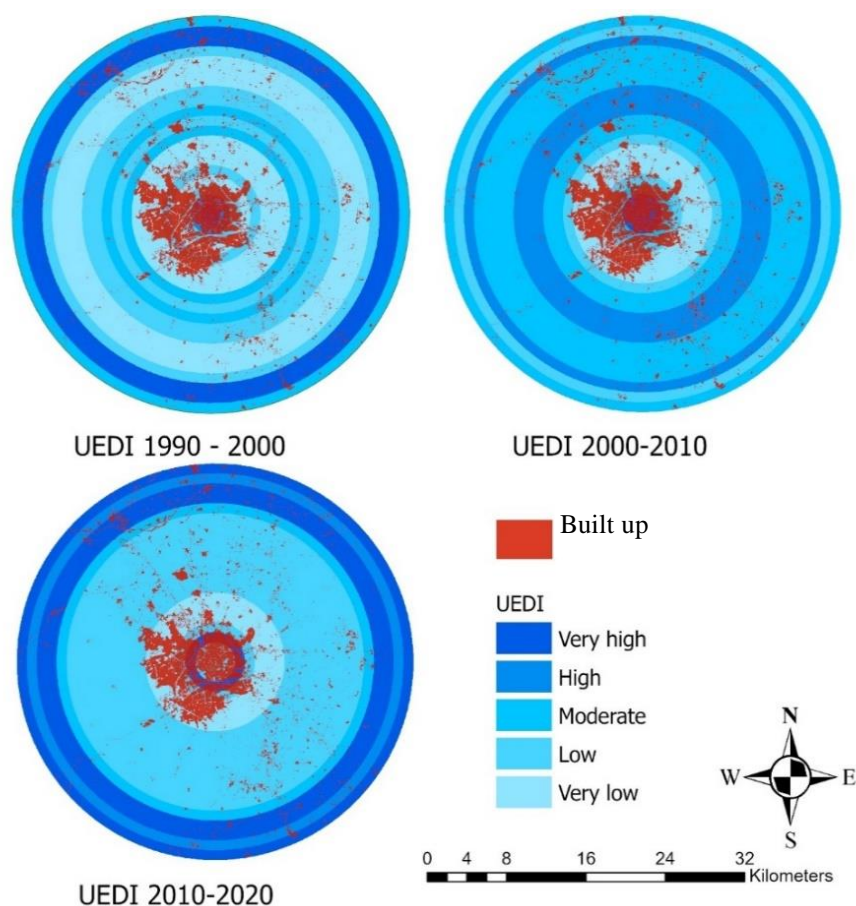


Fig 9. UEDI Index Values in Concentric Regions

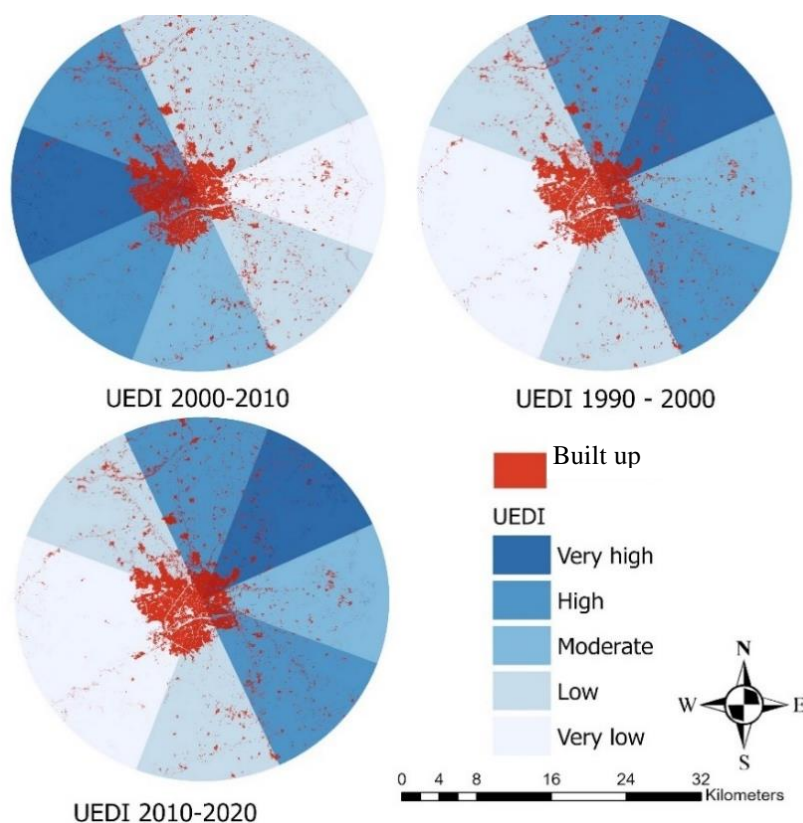


Fig 10. UEDI Index Values in Geographical Directions

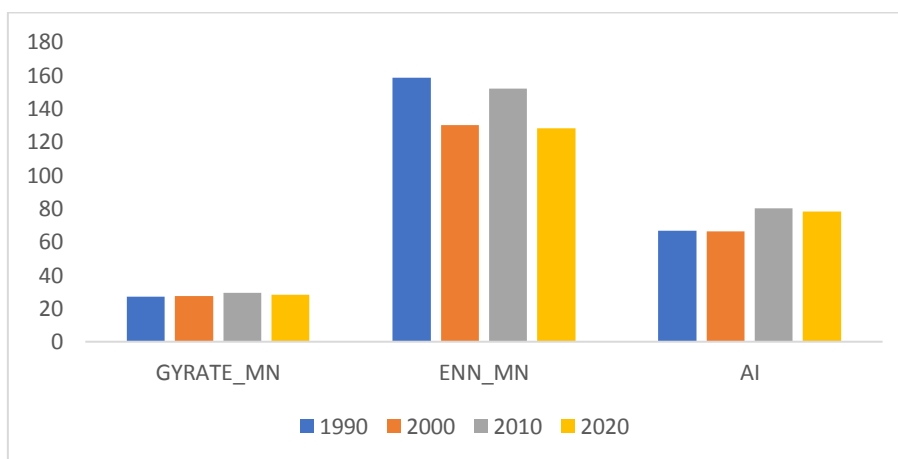


Fig 11. Temporal Changes of Land Spatial Indicators in the Urmia Urban Area

Temporal changes in spatial measures were interpreted in spatial units in order to provide a more comprehensive picture of the pattern of urban expansion in the Urmia urban area. Figure 12 shows the evolution of the cumulative index value for 30 years since 1990. This graph shows a similar negative trend in the cumulative index value in 20 concentric regions over 30

years. The value of the AI index decreased sharply with increasing distance from the city center. Urmia's center sections generally have higher cumulative index values. This could result in the emergence of tiny construction sites in the city's periphery and surrounding areas. This can become a problem if the city grows through dispersed development.

The next graph (Figure 13) of the AI index in the case study in different directions shows how much the ratio of each spatial unit of the accumulation process changed from 1990 to 2020. Overall, according to the graph, a higher value of AI is recorded in the Southeast (SE), South (S), and Southwest (SW) regions. In other words, the patches of land built in these areas have a more cumulative pattern than other areas.

The Gyration index was used in directed and concentric zones to examine the micro

compaction process. The Gyration index value variation in Urmia between 1990 and 2020 is depicted in Figure 14. In general, it is evident that the Gyration Index declined quickly, reaching its minimum value approximately 8 km outside the city center. Then, on the periphery, there has been a consistent tendency. Research has generally indicated that the densification process has been accelerating in Urmia's periphery.

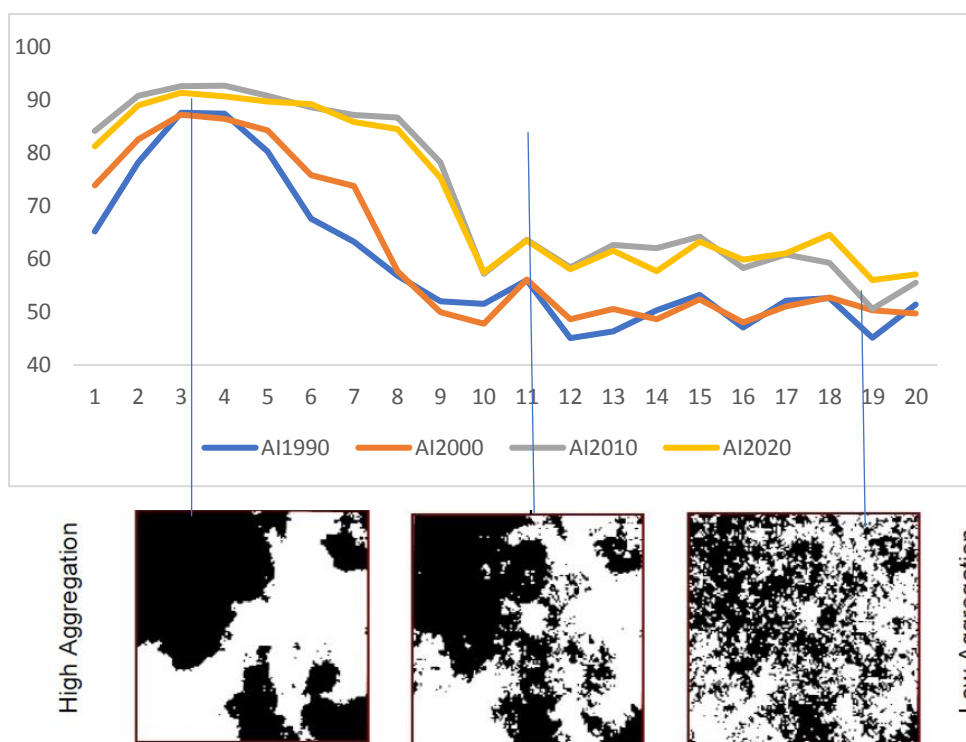


Fig 12. AI index Changes Based on Distance from the City Center

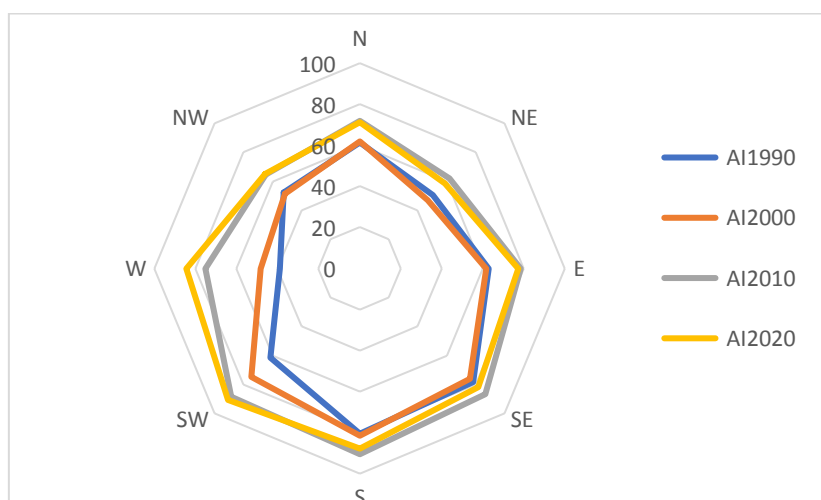


Fig 13. AI Index Changes Based on Geographical Directions

The diagram below (Figure 15) compares the Gyration index in directional zones. This graph shows that in the 1990s-2000s, the eastern (E) and southern (S) regions recorded high values of the gyration index. This process has been similar in the following decades. But, in the following decades, the western part of the region has also witnessed the growth of this index.

The ENN_MN index, which measures the growth in the distance between areas of the same

type of use, was used to examine the next pattern (separation or isolation). The change in ENN_MN in peripheral regions between 1990 and 2020 is depicted in Figure 16's linear diagram. This figure indicates that there is a decrease in the variety of uses as the distance from the city center grows, along with the degree of isolation.

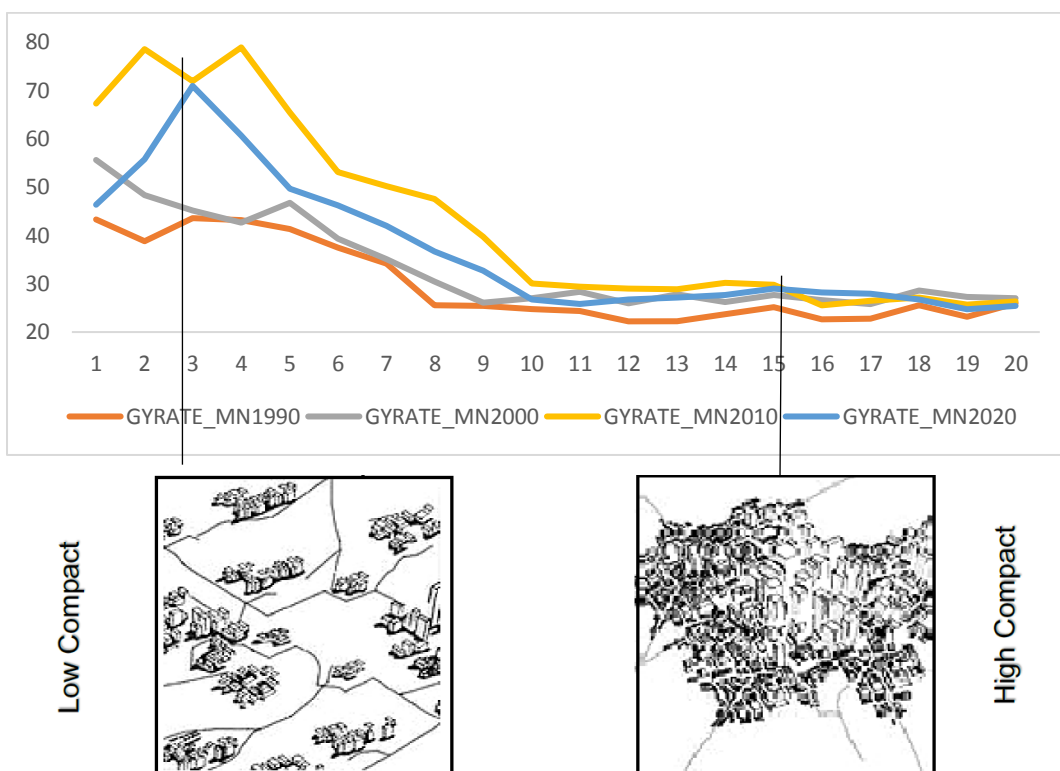


Fig 14. Gyration Index Changes Based on Distance from the City Center

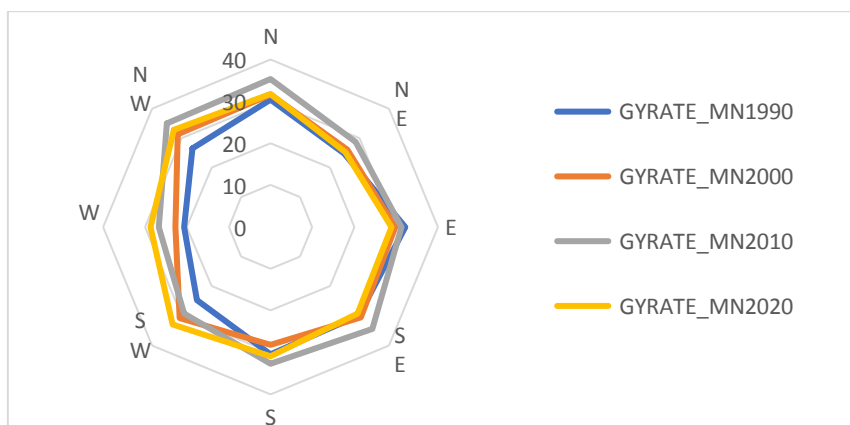


Fig 15. Gyration Index Changes Based on Geographical Directions

The directions with the greatest index values during the research period are displayed in the radar diagram (Figure 17). It is evident that the directional and peripheral zones have higher ENN_MN values overall. Furthermore, the index value in the center regions is significantly lower

than in the periphery regions, and it has exhibited a consistent trend over time. The graphs had identical initial values, but their periphery saw a dramatic increase in value. West (W) and Northeast (NE) have the best separation technique.

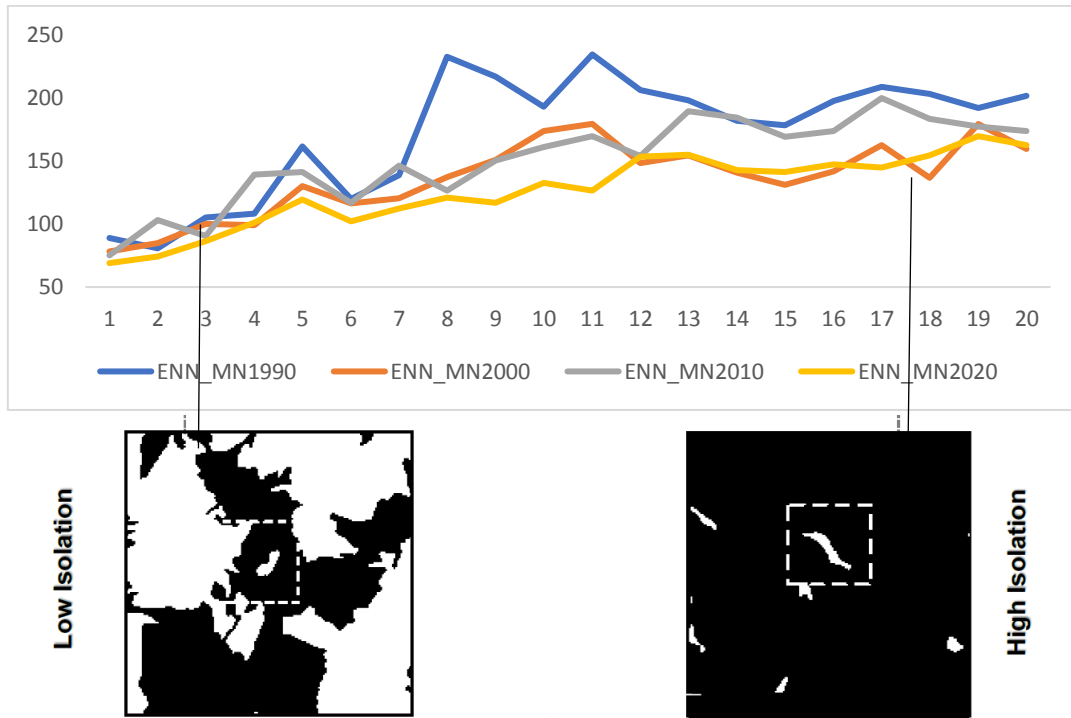


Fig 16. Changes of the ENN_MN Index Based on the Distance from the City Center

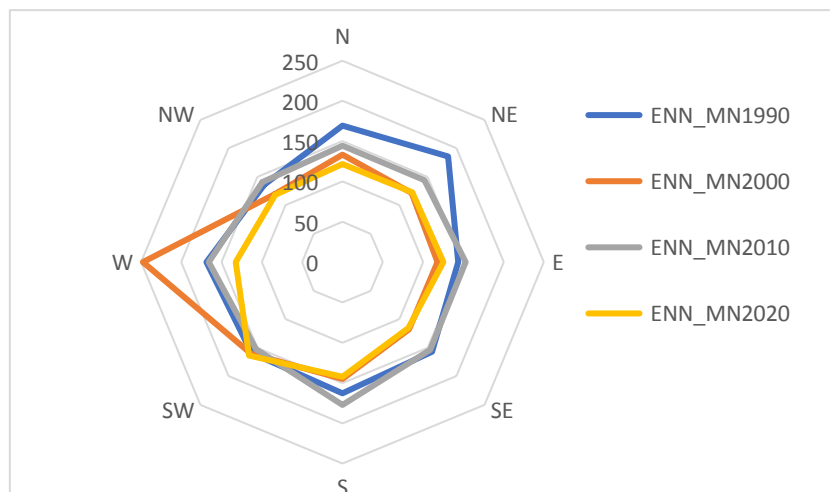


Fig 17. ENN_MN Index Changes Based on Geographical Directions

Two phases can be distinguished when examining Urmia's urbanization. A decline in the AI index indicates that between 1990 and 2000, the city's core area grew due to the rapid expansion in the city's periphery. Furthermore, fresh growth is seen in regions that are divided from one another by open space. It displays the city's sweeping growth. Between 2000 and 2010, there was a decline in the rate of urban expansion. The accumulation of specks fell significantly during this time, and the city saw a cumulative decline in GYRATION_MN. It might suggest that urban patch development has been the main focus of Urmia's ongoing growth, and that this development has been accompanied by a notable rise in ENN_MN and a cumulative decline in Gyration.

Urban Spatial Patterns and the Consequences of Urban Expansion

Two spatial indices (growth ratio indices) for gauging urban expansion are UEII and UEDI, as was previously mentioned. They are regarded as independent factors to look into the connection between spatial patterns and urban growth. Furthermore, the spatial criteria's value is regarded as a dependent variable. The GWR model was selected as a useful model to examine the connection between these two categories of

variables. Table 5 displays the corrected R² and AICt values produced by the GWR model for various time periods. The relatively modest R² values suggest that while the model captures meaningful spatial relationships, urban expansion in Urmia is also influenced by other socio-economic and policy factors not fully represented in the current framework. This limitation should be acknowledged when interpreting the results. In this study, the GWR models yielded only moderate R² values, suggesting that while spatial metrics explain part of the variation, future research should integrate qualitative and socio-economic drivers to more comprehensively capture the dynamics of urban expansion”.

Overall, Table 5 shows higher values for R² and AICt for UEII than for UEDI. The analysis of two distinct variables reveals that the index of urban development exhibits a more robust correlation with spatial patterns. Mapping these coefficients would further enrich the analysis, as it would reveal where spatial associations between expansion intensity and pattern metrics are strongest. While this study presents statistical results, spatial visualization is recommended for future research to strengthen interpretability. To put it simply, alterations in spatial arrangements are strongly correlated with the magnitude of urban expansion.

Table 5. The GWR Regression Measures' Outcomes

Period	Spatial Metrics	Adjusted R ²		AICt	
		UEII	UEDI	UEII	UEDI
1990-2000	AI	0.4571	-0.1402	174.4822	54.6116
	GYRATE_MN	0.4093	0.1429	176.7599	48.9642
	ENN_MN	0.2664	-0.0893	178.6680	53.5632
2000-2010	AI	0.3974	-0.1134	140.6866	87.4393
	GYRATE_MN	0.4646	-0.0422	137.1340	85.4452
	ENN_MN	0.2710	-0.0941	144.4142	86.9415
2020-2010	AI	0.2347	-0.0349	99.7322	73.1597
	GYRATE_MN	0.2488	0.0912	97.8137	70.7454
	ENN_MN	0.1265	0.1703	101.8860	74.1855

The regression coefficients exhibited substantial variation among urbanized locations. The spatial distribution of the coefficient indicates that the connections between spatial factors and UEII values differ across concentric zones. The coefficients for each spatial pattern exhibited a consistent trend for the first two decades, which remained relatively unchanged in the last decade, as illustrated in the accompanying graphs.

The initial graph (Figure 18) depicts the correlation between UEII and AI as influenced by the proximity to the urban core over a span of two decades. Initially, a notable positive association was identified at a distance of 12 km from the city center. This suggests that the acceleration of expansion can result in a rise in the agglomeration process. The negative coefficients observed at a distance of 12 km from the city center indicate that the rapid growth of urbanization results in a decline in the development of larger urban structures and an increase in the consolidation of land in the peripheral areas of Urmia. Mapping the local coefficients would provide an additional layer of insight, allowing visualization of where expansion intensity most strongly correlates with aggregation, dispersion, or isolation patterns. This spatial visualization is recommended for future research to enhance interpretability.

The shift in relationship values between ENN_MN and UEII in the central sections is depicted in the second diagram (Figure 19). Both

positive and negative values have been displayed by the separation index. Over the course of the investigation, a negative correlation has been found overall. It demonstrates how the intensification of urban expansion results in a lessening of the separation process as one moves away from the city center. Conversely, the growth of ENN_MN has been positively impacted by urban expansion. The AI trend line value and the ENN_MN value exhibit a reversing trend when compared.

Figure 20 illustrates how varied oscillations were seen throughout the study period in the effects of expansion on the changes of GYRATION_MN value in various regions. The regions that have suffered the most are 17 km out from the city center. The intensification of urban expansion in region 17 has resulted in a decline in the index of gyration and the dispersion process, as indicated by the negative link between the intensity of expansion and the index of accumulation (Gyration index). Overall, the GWR analysis demonstrated that Urmia City's spatial arrangement may greatly accelerate urban expansion. Although GWR was appropriate for analyzing local spatial variation, complementary regression frameworks such as spatial lag or spatial error models could strengthen the analysis by capturing broader spatial dependencies. Future studies may benefit from integrating these approaches.

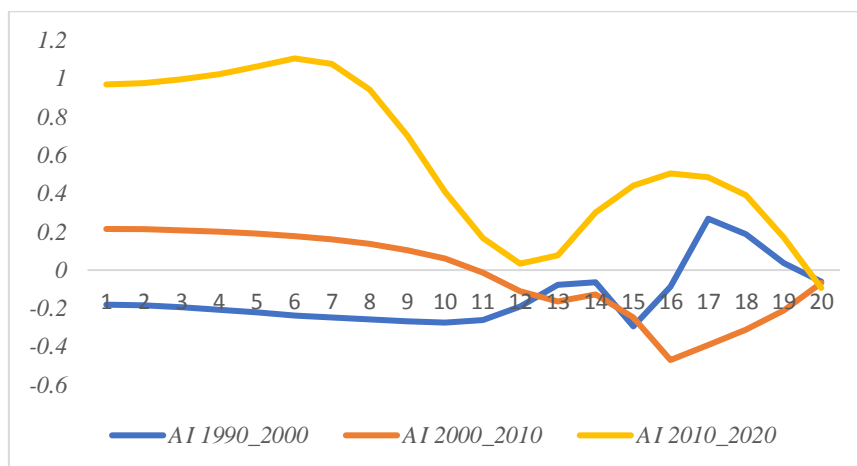


Fig 18. The Relationship Between UEII and AI Based on the Distance from the City Center

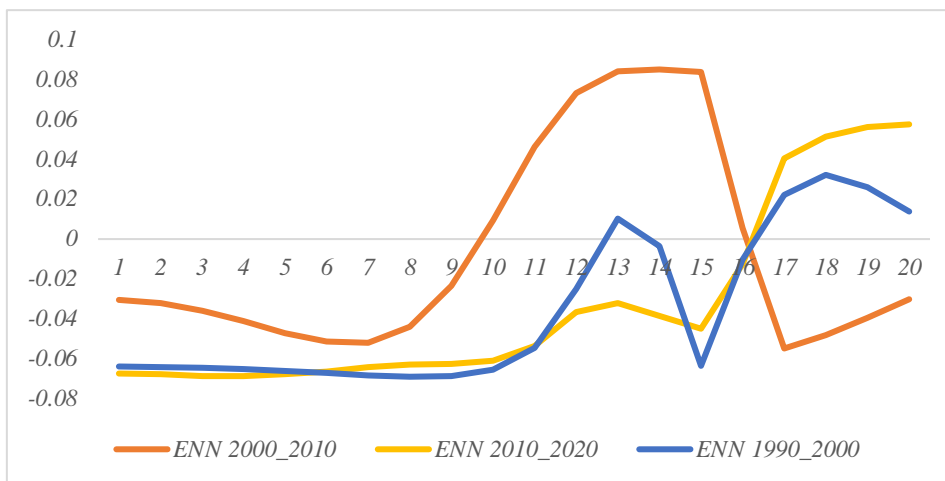


Fig 19. The Relationship between ENN_MN and UEII based on Distance from the City Center

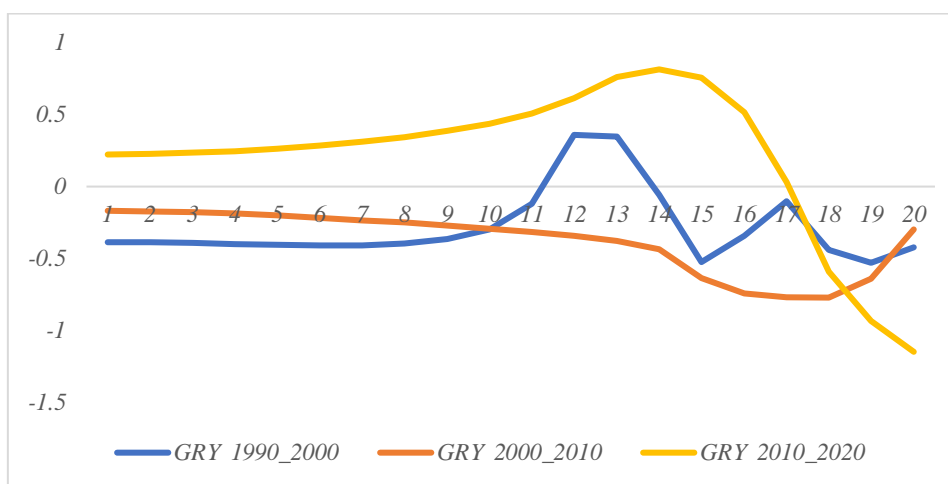


Fig 20. Relationship between GYRATION_MN and UEII based on Distance from the City Center

CONCLUSION

The current study examines the urban expansion of medium-sized cities. In this sense, land use changes were addressed first. The results show that during the course of the four decades under investigation, a variety of factors have influenced changes in land usage. Growing built-up areas and dwindling plant life in Urmia are indicators of the city's increasing urbanization. Rather, the rise in arid areas and the decline in water resources represent changes in the climate and geology of the region. The conversion of desert land into developed land in the Urmia metropolitan area is a good predictor of the effects of urbanization.

Therefore, in the next step, the urban expansion process of Urmia between 1990 and 2020 will be investigated. In this regard, three indicators and two types of boundaries (directional zones and concentric circles) have been used. The results show that the area of Urmia City during the periods under review has been continuously expanded, and the built area has increased proportionately to the total area. Also, the findings indicate that the middle areas of Urimeh city have expanded with high intensity. Compared to the first period (1990-2000), the intensity of expansion has decreased significantly in the following decades. In the first decade of 1990-2000, the greatest difference and intensity of urban expansion occurred in the direction of the

east and north of Urmia city. However, in the next decade, the desire to expand the built lands in the southwest, west, and northwest has increased. Finally, in the decade of 2010-2020, the pattern of urban expansion has tended towards the east and northern regions. The main reason is the increase in agricultural and industrial activities. Linking spatial expansion to sectoral drivers suggests that industrial relocation and agricultural decline are key factors shaping Urmia's urban form. Therefore, urban land-use policies must explicitly integrate agricultural land protection and industrial zoning to reduce unplanned conversions. In the next step, the patterns of the landscape in Urmia city have been examined. In general, the growth of Urmia city has been in the form of scattered and fragmented development. This is quantitatively reflected in the high ENN_MN values at the periphery and the rising MRoG index, which indicates increasing isolation and dispersion of built-up patches. Such evidence highlights the urgency of policies that promote infill development and densification rather than outward sprawl. The results show that the density process has been increasing in the marginal areas of Urmia city. As the distance from the city center increases, segregation also increases, which means a decrease in the variety of uses.

Spatial-geographical regression analysis showed that the spatial pattern of Urmia city can significantly intensify urban expansion.

The results of the present study show that the city of Urmia has experienced urban sprawl in different periods. It confirms the study's results by Abedini et al. (2020). In the discussion of the quantification of growth patterns, the results of the present study show the efficiency of using UEDI, UEII, and AUER indices. This issue is consistent with the results of Heidarinejad's research in 2017 and confirms the suitability of his proposed method for studying the patterns of urban expansion in mid-sized cities.

Examining the characteristics of Urmia's urban growth serves as a useful illustration of Iran's

medium cities. Evidence from the study suggests that urban sprawl has expanded in Urmia city's periphery due to urban expansion. Compared to a more compact pattern, this urban design may result in greater ecological and environmental issues. The dispersed pattern on the outskirts of the city has resulted in a significant loss of agricultural land, making it imperative to improve the efficiency of land management policies and urban land use planning. The study's conclusions lead to the following recommendations:

Infill development policy: considering that Urmia City has many vacant lands (Abedini & Khalili, 2019). The effectiveness of infill policies is directly supported by the aggregation index (AI), which showed higher clustering in southern and southeastern directions. This indicates that compact growth is achievable if vacant plots within the city are prioritized before allowing further expansion. This potential can lead to the optimal use of the existing land and stop the expansion and destruction of the land around the city.

Detailed investigation and monitoring of land use changes: The land use pattern, as one of the most sensitive issues in urban planning, is not only a physical issue but also a social, economic, environmental, and management issue. On the other hand, it should be given sufficient attention in urban development plans, especially the master plan, which is the guiding document for the comprehensive development of the city. For example, the gardens inside Urmia remain neglected for a long time until they turn into barren lands. Finally, these lands will be converted into a built environment. Therefore, it is necessary to control these cases using legal tools such as a comprehensive and detailed city plan. Utilizing green infrastructure, such as including green spaces, parks, and natural corridors in urban plans to improve environmental quality, provide recreational opportunities, and reduce the heat island effect, can be helpful. Creating a green belt can also be

useful for curbing urban expansion and protecting agricultural and natural areas. Lessons from international experiences—such as compact city strategies in East Asia and green belt policies in Europe—can provide valuable guidance. Adapting such practices to the Iranian context could help balance growth with ecological sustainability in medium-sized cities like Urmia.

For future research, it is recommended to consider factors driving urban expansion in different spatial units (directional and concentric zones) according to the spatial extent of the city. Also, the impact of urban expansion on different social groups has shown that urban sprawl has several adverse social effects, such as increasing income inequality, social isolation, and reduced access to public services. However, more research is needed to understand how these effects are distributed across different social groups, such as race, ethnicity, income, and age. Beyond local implications, the case of Urmia aligns with international evidence that unmanaged sprawl in secondary cities undermines climate resilience and food security. Lessons from compact city strategies in East Asia and green belt approaches in Europe may offer transferable insights for Iran's medium-sized cities.

REFERENCES

- Abedini, A., & Khalili, A. (2019). Determining the capacity infill development in growing metropolitans: A case study of Urmia City. *Journal of Urban Management*, 8(2), 316–327. <https://doi.org/10.1016/j.jum.2019.02.005>
- Abedini, A., Khalili, A., & Asadi, N. (2020). Urban sprawl evaluation using landscape metrics and black-and-white hypothesis: A case study of Urmia City. *Journal of the Indian Society of Remote Sensing*, 48, 1021–1034. <https://doi.org/10.1007/s12524-020-01113-3>
- Acheampong, E., Baffoe, G., & Asamoah, E. (2017). Urban expansion in the Greater Accra Metropolitan Area of Ghana: A spatial and temporal analysis. *Land Use Policy*, 67, 506–520. <https://doi.org/10.1016/j.landusepol.2017.06.002>
- Alberti, M. (2008). *Advances in urban ecology: Integrating humans and ecological processes in urban ecosystems*. Springer. <https://doi.org/10.1007/978-0-387-75510-6>
- Al Rifat, S. A., & Liu, W. (2019). Quantifying spatiotemporal patterns and major explanatory factors of urban expansion in Miami Metropolitan Area during 1992–2016. *Remote Sensing*, 11(21), 2493. <https://doi.org/10.3390/rs11212493>
- Alsharif, A. A., & Pradhan, B. (2013). Urban sprawl analysis of Tripoli Metropolitan City (Libya) using remote sensing data and multivariate logistic regression model. *Journal of the Indian Society of Remote Sensing*, 41(2), 431–441. <https://doi.org/10.1007/s12524-012-0227-0>
- Alsharif, A. A. A., Pradhan, B., Mansor, S., & Shafri, H. Z. M. (2015). Urban expansion assessment by using remotely sensed data and the relative Shannon entropy model in GIS: A case study of Tripoli, Libya. *Theoretical and Empirical Researches in Urban Management*, 10(1), 55–71. <http://www.jstor.org/stable/24873521>
- Angel, S., Sheppard, S., Civco, D. L., Buckley, R., Perlin, S., & Herold, M. (2007). *The dynamics of global urban expansion*. Washington, DC: Transportation Research Board.
- Assari, A., Birashk, B., Mousavi Nik, M., & Naghdbishi, R. (2016). Impact of built environment on mental health: Review of Tehran City in Iran. *International Journal on Technical and Physical Problems of Engineering*, 26(1), 81–87.
- Baker, J., Van Der Leeuw, S., & Van Os, B. (2015). Landscape metrics for assessing ecological connectivity and fragmentation. *Ecological Indicators*, 58, 192–198. <https://doi.org/10.1016/j.ecolind.2015.05.040>
- Bouhennache, R., Bouden, T., Taleb, A. A., & Chaddad, A. (2015). Extraction of urban land features from TM Landsat image using the land features index and tasseled cap transformation. In *Recent advances on electro science and computers* (pp. 45–52).
- Botequilha Leitão, A., Miller, J., Ahern, J., & McGarigal, K. (2006). *Measuring landscapes: A*

- planner's handbook*. Washington, DC: Island Press.
- Cheng, J., Zhang, Y., & Li, Z. (2019). A gradient model for land use classification using remote sensing data. *Remote Sensing of Environment*, 231, 111476. <https://doi.org/10.1016/j.rse.2019.111476>
- Clark, P. J., & Evans, F. C. (1954). Distance to nearest neighbor as a measure of spatial relationships in populations. *Ecology*, 35(4), 445–453. <https://doi.org/10.2307/1931034>
- Diggle, P. J. (2013). *Statistical analysis of spatial and spatio-temporal point patterns* (3rd ed.). CRC Press.
- Feyisa, G. L., Mehari, A. S., & Bewket, W. (2014). Water resources assessment using the modified normalized difference water index (MNDWI) at Hare watershed, Eastern Ethiopia. *Journal of African Earth Sciences*, 95, 106–114. <https://doi.org/10.1016/j.jafrearsci.2014.02.011>
- Fotheringham, A. S., Brunson, C., & Charlton, M. (2002). *Geographically weighted regression: The analysis of spatially varying relationships*. Chichester: Wiley.
- Gao, H., Huete, A. R., Ni, W., & Miura, T. (2009). Optical monitoring of large-area snowpack properties and runoff prediction using the MODIS and AMSR-E products. *Remote Sensing of Environment*, 113(12), 2990–3001. <https://doi.org/10.1016/j.rse.2009.08.013>
- Griffith, D. A. (2008). Geographically weighted regression: A method for exploring spatial nonstationarity. *Journal of the Royal Statistical Society: Series B (Statistical Methodology)*, 70(2), 269–291. <https://doi.org/10.1111/j.1467-9868.2007.00642.x>
- He, C., Shi, P., Zhao, S., Li, J., Zhang, X., & Liu, Y. (2015). Urban expansion monitoring in China using Landsat time series data. *Science of the Total Environment*, 502, 533–543. <https://doi.org/10.1016/j.scitotenv.2014.09.081>
- Heidarinejad, N. (2017). *The effects of urban expansion on spatial and socioeconomic patterns of the peri-urban areas: A case study of Isfahan City, Iran* [Master's thesis]. University of Isfahan.
- Herold, M., Scepan, J., & Clarke, K. C. (2015). The use of remote sensing and landscape metrics to describe structures and changes in urban land uses. *Environment and Planning A: Economy and Space*, 34(8), 1443–1458. <https://doi.org/10.1068/a3496>
- Hong, Y. Y., Morris, M., Chiu, C. Y., & Benet-Martínez, V. (2000). Multicultural minds: A dynamic constructivist approach to culture and cognition. *American Psychologist*, 55(7), 709–720. <https://doi.org/10.1037/0003-066X.55.7.709>
- Huete, A. R. (1988). A soil-adjusted vegetation index (SAVI). *Remote Sensing of Environment*, 25(3), 295–309. [https://doi.org/10.1016/0034-4257\(88\)90106-X](https://doi.org/10.1016/0034-4257(88)90106-X)
- Huete, A. R., Tucker, C. J., Kimes, D. S., & Van Leeuwen, W. J. D. (1991). Satellite remote sensing of primary production and water cycle in arid and semi-arid regions. *Remote Sensing of Environment*, 35(3), 217–233. [https://doi.org/10.1016/0034-4257\(91\)90025-L](https://doi.org/10.1016/0034-4257(91)90025-L)
- Huang, B., Zhao, B., Song, Y., Zhang, J., Wang, S., Liu, Z. Z., & Huang, J. (2019). Urban land use mapping using a combination of spectral, spatial and temporal information of Landsat 8 OLI imagery. *International Journal of Applied Earth Observation and Geoinformation*, 78, 251–264. <https://doi.org/10.1016/j.jag.2019.02.016>
- Huang, X., Xia, J., Xiao, R., & He, T. (2019). Urban expansion patterns of 291 Chinese cities, 1990–2015. *International Journal of Digital Earth*, 12(1), 62–77. <https://doi.org/10.1080/17538947.2017.1395090>
- Jones, P., & Kuffer, M. (2023). The overlooked role of secondary cities in sustainable urbanization. *Sustainability*, 15(3), 1221. <https://doi.org/10.3390/su15031221>
- Karimi, A., Molaei, M., & Azizi, M. (2019). Environmental impacts of urban sprawl on agricultural land in Urmia, Iran. *Land Use Policy*, 82, 480–491. <https://doi.org/10.1016/j.landusepol.2019.01.012>
- Li, X., Yeh, A. G. O., & Liu, X. (2020). Analyzing spatial patterns of urban growth using landscape metrics and cellular automata. *Landscape and Urban Planning*, 204, 103938. <https://doi.org/10.1016/j.landurbplan.2020.103938>
- Madanian, M., Azizi, M., & Kheirkhah, M. (2018). The spatial expansion of Tehran metropolitan

- region: Patterns, drivers, and planning implications. *Urban Studies*, 55(12), 2578–2598. <https://doi.org/10.1177/0042098017736171>
- Mirzakhani, N., Behzadfar, M., & Azizi Habashi, S. (2025). Urban expansion modeling using SLEUTH and Cellular Automata–Markov: Case study of Isfahan, Iran. *Environmental Monitoring and Assessment*, 197(3), 110–124. <https://doi.org/10.1007/s10661-025-10123-y>
- Pourafkari, N., Sharifi, A., & Askar, S. (2018). Fragmented urban expansion and ecological risks in Iranian secondary cities. *Cities*, 81, 21–34. <https://doi.org/10.1016/j.cities.2018.03.010>
- Rimal, B., Zhang, L., Keshtkar, H., Haack, B., & Rijal, S. (2017). Monitoring and modeling of urban expansion using Landsat imagery: A case study of Kathmandu, Nepal. *Remote Sensing*, 9(2), 141. <https://doi.org/10.3390/rs9020141>
- Seto, K. C., Güneralp, B., & Hutyra, L. R. (2012). Global forecasts of urban expansion to 2030 and direct impacts on biodiversity and carbon pools. *Proceedings of the National Academy of Sciences*, 109(40), 16083–16088. <https://doi.org/10.1073/pnas.1211658109>
- Seto, K. C., Reenberg, A., Boone, C. G., Fragkias, M., Haase, D., Langanke, T., ... & Simon, D. (2022). Urban land teleconnections and sustainability. *Urban Sustainability*, 2(1), 23–41. <https://doi.org/10.1016/j.urbsus.2022.01.005>
- Sidi, M. (2018). Urban growth, planning challenges, and environmental risks in Iranian medium-sized cities. *Iranian Journal of Urban and Regional Studies*, 10(2), 87–103.
- Terfa, B. K., Chen, N., Liu, D., Zhang, X., & Niyogi, D. (2020). Urban expansion and its impacts on agricultural land in Ethiopia: Evidence from Addis Ababa and secondary cities. *Sustainability*, 12(2), 454. <https://doi.org/10.3390/su12020454>
- Wu, J., Jenerette, G. D., Buyantuyev, A., & Redman, C. L. (2016). Quantifying spatiotemporal patterns of urbanization: The case of Phoenix, USA. *Urban Ecosystems*, 19(1), 295–310. <https://doi.org/10.1007/s11252-015-0472-0>
- You, H., & Yang, X. (2017). Urban expansion patterns and land use efficiency in China's megacities. *Sustainability*, 9(12), 2345. <https://doi.org/10.3390/su9122345>
- Zhao, P., Zhang, M., & Liu, Y. (2019). Understanding urban sprawl in China: The case of Beijing. *Cities*, 92, 1–12. <https://doi.org/10.1016/j.cities.2019.03.006>
- Zhang, Y., Zhao, Y., & Wu, J. (2018). Spatiotemporal evolution of urban land and its driving forces in metropolitan areas of China. *Sustainability*, 10(5), 1301. <https://doi.org/10.3390/su10051301>
- Zhou, Y., & Liu, Y. (2020). Urbanization and sustainable development in China: Spatial analysis of urban expansion and economic growth. *Cities*, 97, 102533. <https://doi.org/10.1016/j.cities.2019.102533>

AUTHOR (S) BIOSKETCHES

A. Ghanabari., *Department of GIS, Faculty of Geography and Planning, University of Tabriz, Tabriz, Iran*

Email: a_ghanbari@tabrizu.ac.ir

A. Khalili., *Department of GIS, Faculty of Geography and Planning, University of Tabriz, Tabriz, Iran*

Email: amin.khalili89@gmail.com

B. Feizizadeh., *Department of GIS, Faculty of Geography and Planning, University of Tabriz, Tabriz, Iran*

Email: feizizadeh@tabriz.ac.ir

HOW TO CITE THIS ARTICLE

Ghanabari, A., Khalili, A., Feizizadeh, B. (2026). Examining the Impacts of Urban Expansion on Spatial Patterns of Rurban Space Case Study: Urmia City. *Int. J. Architect. Eng. Urban Plan*, 36(1): 1-30, <https://dx.doi.org/10.22068/ijaup.837>.

URL: <http://ijaup.iust.ac.ir>

